The International George Papatheodorou Symposium

Patras, September 17–18, 1999

Proceedings

FAST ION CONDUCTING GLASSES

C.P. Varsamis, E.I. Kamitsos and G.D. Chryssikos
Theoretical and Physical Chemistry Institute,
National Hellenic Research Foundation,
48 Vass. Constantinou Ave., Athens 116 35, Greece

AgI-doped fast ion conducting borate glasses xAgI-(1-x)[Ag_2O-nB_2O_3] (n=2, 0.5) in bulk and thin film forms were studied by infrared spectroscopy. The short-range order structure of the network was found to be directly affected by AgI, and this was accounted for by isomerisation and disproportionation reactions between triangular and tetrahedral borate species for the diborate (n=2) and pyroborate (n=0.5) families, respectively. This effect is reflected in the decrease of the glass transition and fictive temperature upon AgI addition. Analysis of the transmission spectra of thin films for diborate glasses showed that optical and thermal history effects lead to spectral differences between thin films and bulk samples. Far-infrared analysis for pyroborate glasses revealed two distinct environments for silver ions formed by oxygen atoms and iodide anions. At high AgI contents the silver-iodide sites are probably growing into AgI-like clusters. In the diborate family the presence of a range of oxide, iodide and mixed O/I environments for silver ions is supported by the far-infrared data. Thus, the nature of sites exploited by silver ions in AgI-containing borate glasses depends on both Ag_2O and AgI content.

Introduction

Fast ion conducting (FIC) glasses are challenging materials due to their high ionic conductivity and the possibility for applications in electrochemical devices [1-3]. AgI-doped borate glasses xAgI-(1-x)[Ag_2O-nB_2O_3] have been widely studied as model FIC systems. These glasses are stable, exhibit high ionic conductivity and can be prepared easily in a wide glass-forming region [4,5]. Despite the numerous studies devoted to such glasses, their structure and ion conduction mechanism are still a subject of debate [6-15].

It has been suggested that the short-range order (SRO) of the borate network changes in a systematic way upon increasing the amount of AgI while keeping the Ag_2O/B_2O_3 ratio constant [5,6], while other studies indicate that AgI addition does not induce modifications of the SRO of the glass [7-9]. The state of AgI in the borate network and its effect on the ion transport process are also matters of controversy. It has been proposed that AgI forms a pseudophase within the glass matrix, and that silver ions migrate along pathways established by iodide ions [1,10,11]. On the contrary, other studies suggest that AgI is dispersed in interstices of the host matrix [9,12,13], and that the conductivity enhancement is due to the expansion of the glass network caused by AgI-doping [14,15].

The purpose of this paper is to investigate both the network structure and the silver ions hosting sites by infrared (IR) reflectance and transmittance spectroscopy of two families of xAgI-(1-x)[Ag_2O-nB_2O_3] glasses; with n=2 (diborate) and n=0.5 (pyroborate). Analysis of the mid-IR spectra reveals details of the SRO of the borate network, while the far-IR profiles yield information on the nature of sites hosting silver cations. The simultaneous analysis of transmittance and reflectance spectra allows comparison of the results of the two different techniques, in relation with the findings of previous works reported in the literature [6,8].

Experimental

Glasses were prepared using stoichiometric amounts of reagent grade AgI, $AgNO_3$ and B_2O_3, mixed in Pt crucibles and heated at 650°C until the NO_x gas had dissipated. Then, the mixture was melted at 850-950°C for 25-30 min, depending on composition. Bulk samples for specular reflectance measurements were obtained by splat quenching techniques in the composition range $0 \leq x \leq 0.65$ for the diborate, and $0.4 \leq x \leq 0.6$ for the pyroborate family. From the same batch used to prepare the bulk samples, thin films were obtained in the diborate family only for $0.1 \leq x \leq 0.60$ by employing the procedure described by Liu and Angell [16].

Infrared spectra were measured on a Fourier-transform vacuum spectrometer (Bruker 113v) in the range 25-5000 cm^{-1}. Specular reflectance spectra were measured in an 11° off-normal mode and transmittance spectra were recorded with the plane of the film placed normal to the incident beam.

Results and discussion

Infrared spectra of bulk samples

The specular reflectance spectra of bulk samples were analyzed by the Kramers-Kronig transformation to calculate the absorption coefficient spectra, α(ν). The α(ν) spectra of xAgI-(1-x)[Ag_2O-$2B_2O_3$] glasses reported in Fig.1 are dominated in the mid-IR region by strong absorption envelopes at *ca.* 1350 and 1000 cm^{-1}. These features are attributed to the asymmetric stretching mode of borate triangles $B\emptyset_3$ and $B\emptyset_2O^-$ (1350 cm^{-1}) and tetrahedral units, $B\emptyset_4^-$ (1000 cm^{-1}), respectively (Ø=oxygen atom bridging two boron atoms) [6,17]. Though the AgI content varies in a rather broad range, $0 \le x \le 0.65$, such spectra have quite similar bandshapes, suggesting that AgI addition does not cause the formation of new structural units in the borate network,. However, it is noted that AgI addition induces a change in the relative intensities of the envelopes at *ca.* 1350 and 1000 cm^{-1} in favor of the latter, suggesting the occurrence of AgI-induced structural rearrangements mostly related to changes in the relative population of triangular and tetrahedral borate units. The short-range order (SRO) of the binary $Ag_2O{\cdot}2B_2O_3$ glass contains $B\emptyset_3$ and $B\emptyset_2O^-$ triangular units and $B\emptyset_4^-$ tetrahedra [18]. To quantify the network structure of AgI-doped diborate glasses the fractions X_3, X_2 and X_4 of the local structural units $B\emptyset_3$, $B\emptyset_2O^-$ and $B\emptyset_4^-$, respectively, were calculated. For this purpose we employed the recently introduced model [19,20] that involves the deconvolution of absorption profiles (see inset of Fig.1) and the assignment of component bands to borate polyhedra. In Fig.2 are reported the calculated fractions X_2 and X_4 as a function of AgI content, with X_3 being composition independent (X_3=0.5). As x increases from 0 to 0.65, X_4 varies from 0.34 to 0.39, while X_2 from *ca.* 0.16 to 0.11 and these changes are considerably larger than the estimated experimental error (*ca.* 3%). The result for the $Ag_2O{\cdot}2B_2O_3$ glass (X_4=0.34) is in excellent agreement with the corresponding value obtained from NMR spectroscopic data (N_4=0.35) [21].

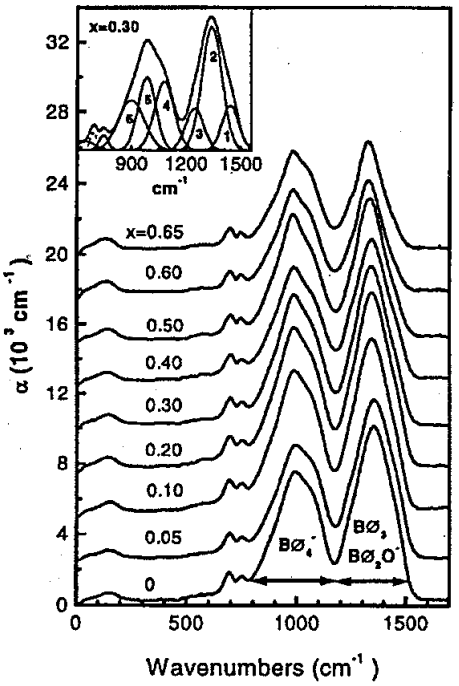

Fig.1: α(ν) spectra of xAgI-(1-x)[Ag_2O-$2B_2O_3$] glasses. The spectra have been offset by 2.5×10^3 cm^{-1} to allow comparison. The inset shows example of deconvolution of an absorption spectrum into Gaussian component bands.

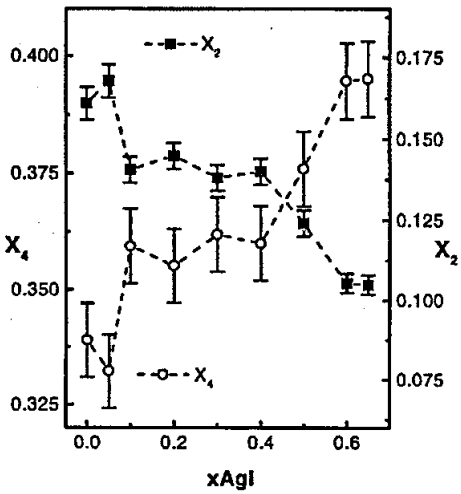

Fig.2: Fractions X_4 and X_2 of borate tetrahedra ($B\emptyset_4^-$) and triangles ($B\emptyset_2O^-$), respectively, as a function of AgI content in xAgI-(1-x)[Ag_2O-$2B_2O_3$] glasses.

These results demonstrate the effect of AgI on the SRO of the glass, and this can be understood in terms of the chemical equilibrium between the isomeric $B\emptyset_2O^-$ and $B\emptyset_4^-$ units:

$$B\emptyset_4^- \rightleftarrows B\emptyset_2O^- \qquad (1)$$

The fractions reported in Fig.2 show that AgI addition shifts the equilibrium to the left. This SRO change can be quantified by estimating the quasi-equilibrium constant, K_{eq}, at constant pressure for reaction (1):

$$K_{eq} = X_2 / X_4 \qquad (2)$$

It was found that K_{eq} and the corresponding glass transition temperature, T_g, of diborate glasses show the same dependence on AgI content [20]. Such an interrelation between T_g and SRO allowed us to estimate, from the slope of the $\ln K_{eq}$ vs. $1/T_g$ plot, the enthalpy change associated with reaction (1), ΔH=32 ± 5 kJ/mol of boron. This result is in good agreement with reported data for the reaction $B\emptyset_4^- \rightleftarrows B\emptyset_3$ + NBO in sodium borate melts (ΔH=35 ± 12 kJ/mol of boron, NBO = non-bridging oxygen) [22].

The corresponding α(ν) spectra of pyroborate glasses, xAgI-(1-x)[Ag_2O-0.5B_2O_3], were found to be dominated by strong envelopes at *ca.* 955, 1030, 1245 and 1315 cm^{-1} [19]. These features manifest the presence of borate tetrahedra, $B\emptyset_4^-$ (955 and 1030 cm^{-1}), orthoborate triangles, BO_3^{3-} (1245 cm^{-1}), and pyroborate units, $B_2O_5^{4-}$ (1315 cm^{-1}) [17]. Though in pyroborate glasses the fractions cannot be determined unambiguously [20], it was found that AgI affects the relative intensity of mid-IR bands. In particular, all glasses present strong bands due to $B\emptyset_4^-$ tetrahedra, despite the fact that the fraction of $B\emptyset_4^-$ units is negligible in binary pyroborate glasses [17]. Thus, the effect of AgI in the pyroborate family can be related to the co-existence of $B_2O_5^{4-}$, BO_3^{3-} and $B\emptyset_4^-$ species, according to the disproportionation reaction:

$$B_2O_5^{4-} \rightleftarrows BO_3^{3-} + B\emptyset_4^- \qquad (3)$$

It appears that the presence of AgI results in the stabilization of pyroborate species, even though the corresponding silver-pyroborate crystal or glass (Ag_2O-0.5B_2O_3) can not be synthesized to the best of our knowledge.

Infrared spectra of thin films

Transmittance spectra of thin films in the diborate family are reported in Fig.3 and show the same absorption features as the corresponding bulk samples (Fig.1). In addition, these spectra exhibit interference fringes above *ca.* 1500 cm^{-1} where the films become quasi-transparent, which extend also to lower frequencies and overlap with the absorption peaks of the glass network. Hence, a careful analysis of the transmittance spectral data requires taking into account the interference pattern.

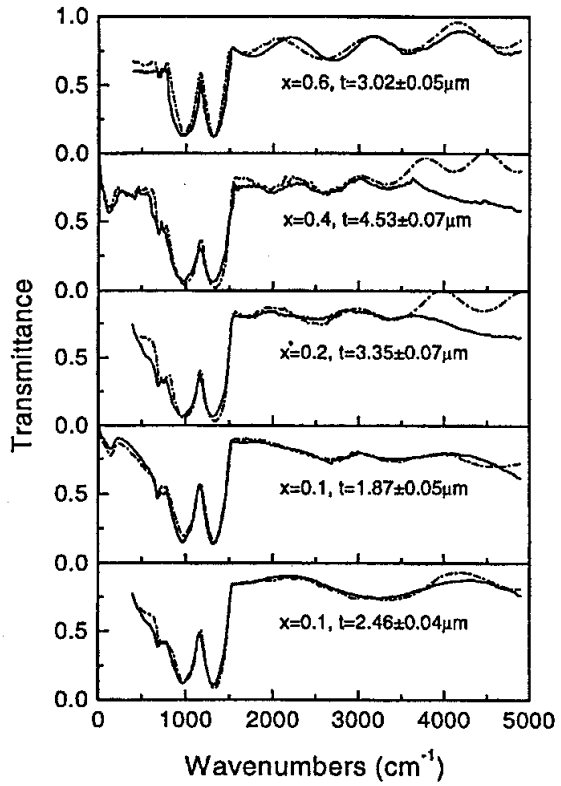

Fig.3: Typical infrared transmission spectra of films with different AgI contents in the diborate family xAgI-(1-x)[Ag_2O-2B_2O_3]. Solid lines indicate experimental spectra and dash dotted lines are the best fits to the experimental spectra [20]. The thickness of films obtained by the fitting procedure is also given.

Transmittance spectra, T(ν), were simulated by using a rigorous expression which depends on the real, n(ν), and imaginary, k(ν), parts of the complex refractive index and on the thickness, d, of the film [23]. As discussed in detail elsewhere [20] the n(ν) and k(ν) functions obtained by the Kramers-Kronig transformation of the bulk sample reflectivity can be employed to fit the experimental T(ν) spectra having the film thickness as the only variable parameter. Typical results of the simulation are shown in Fig.3 for comparison with the experimental spectra. It turns that an appropriate analysis of optical measurements on thin films leads to similar conclusions for the SRO structure. It should be mentioned however that the crucial parameter in the case of thin film analysis is the film thickness. In fact, the measured spectrum of a finite film is a convolution of the spectrum of a semi-infinite sample and the constructive interference due to multiple reflections between the two interfaces of the film. Such interference introduces an oscillatory term with period and amplitude dependent on thickness, which can alter the shape of the spectrum in a rather complicated way controlled by film thickness [20]. So, a quantitative comparison between the results obtained on bulk and thin film samples can be made only when the latter are carefully analyzed to eliminate the dependence on the film thickness.

In addition, it is underlined that samples in bulk and thin film forms of the same composition may have different fictive temperatures due to their different thermal histories. This affects directly equilibrium (1) and consequently the SRO structure of the glass. While, bulk samples were obtained by splat quenching the melt immediately after removal from the furnace, thin films were blown from a melt

drop that was cooled to obtain an appropriate viscosity. It follows that thin films may have lower fictive temperatures compared to bulk samples, and larger X_4 according to equilibrium (1). This may also explain the observed small differences between experimental and simulated spectra in Fig.3.

Far-IR spectra of xAgI-(1-x)[Ag_2O-nB_2O_3] glasses

In Fig.4 are shown the expanded far-IR absorption coefficient profiles of xAgI-(1-x)[Ag_2O-nB_2O_3] glasses. These are dominated by a broad asymmetric profile due to the vibration of Ag cations in their hosting sites [6,20]. The nature of cationic sites can be studied by deconvoluting the far-IR spectra into Gaussian component bands. Typical deconvolution results by using the minimum number of components are included in Fig.4. The binary silver diborate glass (x=0) was fitted by three component bands at *ca.* 52 (ν_L), 145 (ν_H) and 272 cm^{-1}, as in previous studies [18]. The ν_L and ν_H bands are attributed to Ag-O vibrations in oxide environments and the third component is assigned to a deformation mode of the borate network [18,19]. The profiles of AgI-containing diborate glasses were fitted also with three components (Fig.4), with frequencies between 45-50 cm^{-1} (ν_L), 128-146 cm^{-1} (ν_H) and 266-272 cm^{-1}. AgI addition results in the relative increase of the intensity of the ν_H band, and in the progressive shift of its frequency towards lower values (146 cm^{-1} for x=0 to 125 cm^{-1} for x=0.65).

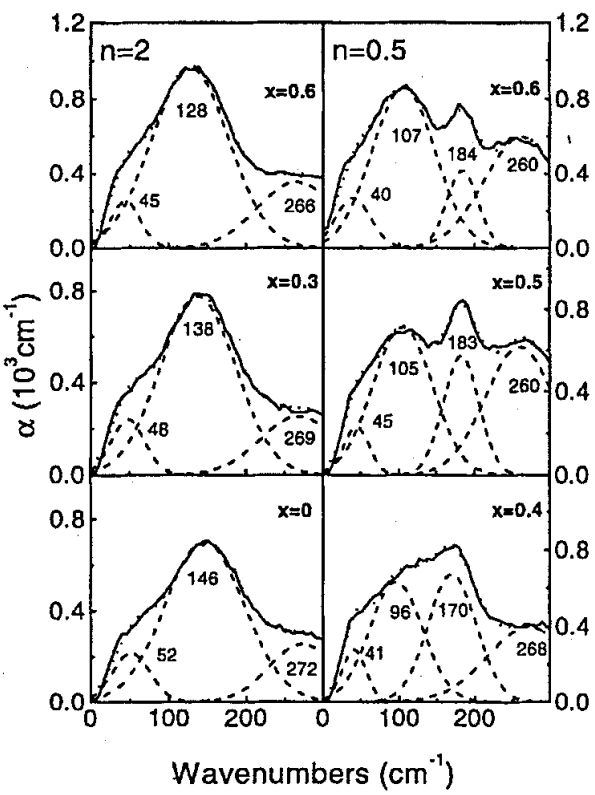

Fig.4: Far-infrared spectra (solid lines) of xAgI-(1-x)[Ag_2O-nB_2O_3] glasses with n=2, $0 \le x \le 0.6$ (diborate) and n=0.5, $0.4 \le x \le 0.6$ (pyroborate), deconvoluted into Gaussian component bands (dashed lines). The simulated spectra are shown by dotted lines.

The pyroborate far-IR spectra present remarkable differences compared to the diborate ones and were described by four distinct components. Three components at *ca.* 40, 175 and 260 cm^{-1} are analogous to those found in the diborate family, while the one at *ca.* 100 cm^{-1} is a new feature. This new component increases in intensity and shifts to higher frequencies upon AgI addition, suggesting that it could be assigned to vibrations of Ag cations in primarily iodide environment [6,20]. This assignment is further supported by the fact that crystalline AgI has a strong infrared absorption at *ca.* 110 cm^{-1}, attributed to the Ag-I stretching mode, ν_{Ag-I}, in a tetrahedral environment of I^- anions [24]. The increase of ν_{Ag-I} frequency from 96 cm^{-1} (x=0.4) to 107 cm^{-1} (x=0.6) may indicate a progressive organization and growth of silver iodide sites into a separate AgI-like pseudophase though its size cannot be estimated from the present infrared data. However, a recent field emission scanning electron microscopy study of orthoborate glasses 0.75AgI-0.25[Ag_2O-$0.33B_2O_3$] revealed the presence of AgI-rich amorphous particles with diameter 40-60 nm [25].

In view of the above results, the downshift of ν_H upon AgI addition in diborate glasses can be explained in two ways. First, the band with frequency ν_H is assumed to be a convolution of two bands, at *ca.* 146 cm^{-1} (oxide band) and 110 cm^{-1} (iodide band). AgI addition enhances the intensity of the latter band and the peak maximum of the convoluted band shifts naturally towards lower frequency values. A second explanation is based on a progressive substitution of oxygen by iodide ions in the coordination sphere of Ag cations as x increases. This would lead to the formation of mixed oxyiodide sites, and the combined effect of the increasing reduced mass and the decreasing force constant would be a net decrease of ν_H with AgI addition [20]. Both models, i.e. (a) formation of separate Ag-oxide and Ag-iodide sites, and (b) formation of mixed Ag-O/I environments, predict the observed trend of ν_H with AgI addition. It appears that for the diborate family an intermediate situation is perhaps more realistic for the nature of sites occupied by silver cations.

Concluding remarks

Superionic borate glasses $xAgI-(1-x)[Ag_2O-nB_2O_3]$ in bulk and thin film forms were studied by infrared spectroscopy to investigate the short-range order (SRO) of the network and the nature of sites occupied by silver ions.

The network structure of diborate glasses (n=2) was found to consist of $B\emptyset_2O^-$ and $B\emptyset_3$ triangles and $B\emptyset_4^-$ tetrahedra. The calculated fractions of $B\emptyset_2O^-$ and $B\emptyset_4^-$ units, X_2 and X_4, depend on AgI content and this was explained in terms of the equilibrium $B\emptyset_4^- \rightleftarrows B\emptyset_2O^-$. This direct influence of AgI on the SRO of glass was correlated with the glass transition and fictive temperature at which the supercooled liquid is frozen into the glassy state. Similarly, pyroborate glasses (n=0.5) contain orthoborate triangles, BO_3^{3-}, pyroborate dimers, $B_2O_5^{4-}$, and $B\emptyset_4^-$ tetrahedra. AgI addition was found to favor the reaction $B_2O_5^{4-} \rightleftarrows BO_3^{3-} + B\emptyset_4^-$, and to lead to the stabilization of pyroborate species in the glassy state.

The study of the transmittance spectra of thin films in the diborate composition showed that a direct comparison between bulk samples and thin films should be avoided. This is due to the fact that the shape of the transmittance spectra of films depends on both film thickness and differences in thermal history between bulk samples and films.

The far-IR analysis of pyroborate glasses revealed the presence of distinct oxide and iodide environments for silver ions, without excluding the presence of silver sites with mixed O/I coordination. It was also found that an AgI-like pseudophase might develop at high AgI contents. In the diborate family the situation is rather complicated and a realistic scenario involves the existence of a range of sites for silver cations, i.e. oxide, iodide and mixed oxyiodide sites. Thus, the nature of silver ionic sites appears to depend on both Ag_2O/B_2O_3 ratio, i.e. the degree of modification of the borate network, and AgI content.

References

[1] T. Minami, *J. Non-Cryst. Solids* **73**, 273 (1985).
[2] C.A. Angell, *Ann. Rev. Phys. Chem.* **43**, 693 (1992).
[3] M.D. Ingram, *Current Opinion in Solid State and Materials Science* **2**, 399 (1997).
[4] A. Magistris, G. Chiodelli, A. Schiraldi, *Electrochim. Acta* **23**, 585 (1978).
[5] T. Minami, Y. Ikeda, T. Tanaka, *J. Non-Cryst. Solids* **52**, 159 (1982).
[6] E.I. Kamitsos, J.A. Kapoutsis, G.D. Chryssikos, J.M. Hutchinson, A.J. Pappin, M.D. Ingram, J.A. Duffy, *Phys. Chem. Glasses* **36**, 141 (1995).
[7] G. Chiodelli, A. Magistris, M. Villa, J.L. Bjorkstam, *J. Non-Cryst. Solids* **51**, 143 (1982).
[8] J.J. Hudgens, S.W. Martin, *Phys. Rev. B* **53**, 5348 (1996).
[9] J. Swenson, L. Borjesson, R.L. McGreevy, W.S. Howells, *Phys. Rev. B* **55**, 11236 (1997).
[10] G. Carini, M. Cutroni, M. Frederico, G. Galli, G. Tripodo, *Phys. Rev. B* **30**, 7212 (1984).
[11] C. Rousselot, J.P. Malugani, R. Mercier, M. Tachez, P. Chieux, A.P. Pappin, M.D. Ingram, *Solid State Ionics* **78**, 211 (1995).
[12] G. Licheri, A. Musinu, G. Paschina, G. Piccaluga, G. Pinna, A. Magistris, *J. Chem. Phys.* **85**, 500 (1986).
[13] F. Rocca, G. Dalba, P. Fornasini, A. Tomasi, *Solid State Ionics* **53-56**, 1253 (1992).
[14] J. Swenson, L. Borjesson, *Phys. Rev. Lett.* **77**, 3569 (1996).
[15] J. Swenson, L. Borjesson, *J. Non-Cryst. Solids* **232-234**, 658 (1998).
[16] C. Liu, C.A. Angell, *J. Chem. Phys.* **93**, 7378 (1990).
[17] E.I. Kamitsos, A.P. Patsis, G.D. Chryssikos, *J. Non-Cryst. Solids* **152**, 246 (1993).
[18] J.A. Kapoutsis, E.I. Kamitsos, G.D. Chryssikos, in *Borate Glasses Crystals and Melts*, Eds. A.C. Wright, S.A. Feller and A.C. Hannon, Soc. Glass Technology (1997) p.p. 303-312.
[19] C.P. Varsamis, E.I. Kamitsos, G.D. Chryssikos, J.A. Kapoutsis, in *Proc. 18th Inter. Congress on Glass*, Eds. M.K. Choudham, N.T. Huff and C.H. Drummond (Am. Ceram. Soc. 1998) p.p. 39-44.
[20] C.P. Varsamis, E.I. Kamitsos, G.D. Chryssikos, *Phys. Rev. B* in press.
[21] K.S. Kim, P.J. Bray, *J. Non-Cryst. Solids* **111**, 67 (1989).
[22] S. Sen, Z. Xu, J.F. Stebbins, *J. Non-Cryst. Solids* **226**, 29 (1998).
[23] S. Cunsolo, P. Dore, C.P. Varsamis, *Appl. Optics* **31**, 4554 (1992).
[24] G. Burns, F.H. Dacol, M.W. Shafer, *Phys. Rev. B* **16**, 1416 (1977).
[25] M. Tatsumisago, N. Itakura, T. Minami, *J. Non-Cryst. Solids* **232-234**, 267 (1998).